

## SIMULATION OF OIL EXTRACTION IN COUNTER-CURRENT CROSSED FLOWS WITH THE USE OF ARTIFICIAL NEURAL NETWORKS

### G. C. Thomas

UNIJUI – Northwest Regional University of Rio Grande do Sul,  
Department of Mathematic, Physics and Statistics, CP 560, CEP 98.700-000, Ijuí – RS – Brazil  
[gctomas@uol.com.br](mailto:gctomas@uol.com.br)

### V. G. Krioukov

UNIJUI – Northwest Regional University of Rio Grande do Sul, Master Degree Program  
in Mathematical Modeling, CP 560, CEP 98.700-000, Ijuí – RS – Brazil  
[kriukov@admijui.unijui.tche.br](mailto:kriukov@admijui.unijui.tche.br)

### H. A. Vielmo

UFRGS – Federal University of Rio Grande do Sul  
Graduate Program in Mechanical Engineering, 90050-170, Porto Alegre – RS - Brazil  
[vielmoh@mecanica.ufrgs.br](mailto:vielmoh@mecanica.ufrgs.br)

**Abstract.** *A new mathematical model of processes in a “Rotocell” extractor was developed. The model considers: a two-dimensional approach of counter-current crossed flows with oil diffusion along miscela; mass transfer between the bulk, pore and solid phases; the effect of the existing processes in the drainage and loading zones; oil loss and variation in the miscela viscosity and density. The model leads to a system of coupled partial and ordinary differential equations, which is solved with the neural network approach. The solution is compared with experimental data and with the method of ideal stages. The numerical simulations reveal the extraction field properties in the transient regimes.*

**Keywords:** *Vegetable Oil, Extraction, Mathematical Model, Neural Network, Counter-Current Crossed Flows, Porous Media.*

### 1. Introduction

The mathematical modeling of processes in nutritious industry is a subject that receives continuing attention in the open literature. In the present work, this approach is applied to industrial extractors that are extensively employed in sugar, oil and coffee processing. In general, they are managed by the principle of counter-current crossed flows (CCC), of the raw material (a porous media that contains the substance to be extracted - for instance, oil) and miscela. Inside the extractor, the flows of miscela and the raw material interact so that, in the outlet, the raw material has low oil concentration, and miscela has high oil concentration. The most used extractors are: Rotocell, De-Smet and Crown-Model (Bockish, 1998). Several multi stage methods (Foust et al, 1982) are being used to design and simulate the extractor processes. In their methods, uniform oil concentrations in percolation sections and the equilibrium between bulk and pore phases are assumed. But as indicated by Bewaji & Best (1996), actually is demanded modeling more detailed with: space concentration distributions, considering: extraction field diffusion, non-equilibrium mass transfer etc.

Several articles were considered to the mathematical modeling of vegetable oil extraction. Karnofski (1986) proposed a semi-empiric model of the oil extraction in industrial extractors that is based on the following considerations: the oil retention time is determined by the solution rate; the resistance to the oil diffusion through the flake borders is relatively small. The model employed experimental results, which were extended for the prediction of oil loss in industrial extractors. In work (Abrahamm et al, 1988), the coupled mathematical model of an extractor with other plant equipment was presented (dissolventizer, miscela separator, etc). The model included algebraic equations for each flow component (marc, water, oil and solvent) that considers the balance between the phases. The extractor sub-model was based on the multi-stage method that uses experimental data, and does not have the objective of presenting oil concentration distribution in the extraction field. A significant step was achieved by Majundar et al. (1995), which developed the oil extraction model in an fixed bed of expanded flakes (Bockish, 1998) which contrarily to the laminated flakes, present the best extraction properties. This system was treated as a porous medium with two porosity types (bulk and pore). The equilibrium constant concept was used between the solid and pore phases.

However, it is not available in the literature, a coupled model of CCC flows that considers: spatial distributions of oil concentration in the extraction field; mass transfer and diffusion; the presence of trays, and of the loading and drainage zones. In this paper, a model was developed for a “Rotocell” extractor whose scheme is presented in Fig. (1). The main components involved in the extraction are: the expanded flakes, the miscela and the oil. The raw material is a porous medium made of grains (for instance, soy), which is characterized by two types of porosity,  $\varepsilon_b$  (the external porosity or channeled spaces) and  $\varepsilon_p$  (the internal porosity or cavity spaces), and is modeled as porous particles with diameter  $d_p$ . The solid part of the particles, named as solid phase, can also contain an oil portion. Miscela is a liquid that, in contact with flakes, extracts oil. In spaces  $\varepsilon_b$ , miscela is called bulk phase and in spaces  $\varepsilon_p$  - pore phase. In the extractor inlet, the miscela has a very small oil concentration ( $C_{in}$ ), and is called solvent or weak miscela.

In the outlet, it is called concentrated miscela. The oil initially is contained in the raw material; the objective of the extraction process is to transfer this species to the miscela.

The main elements of the Rotocell extractor, are shown in Fig. (1). For operational reasons, the extractor is separated into 3 areas: loading - 8, extraction (space between wagons 8 and 6) and drainage - 12. In the loading area, the wagon is loaded with both raw material and concentrated miscela. The wagons move evenly from direction 2 to 11, returning to position 2 to complete the cycle. As observed, the extractor is rounded. The extraction area is divided into percolation sections; each section corresponds to two wagons. The wagon moves under the vertical flows of miscela that extract the oil from the flakes. Miscela passes from tube 4 to 5 in counter-current crossed flow (relatively to the raw material flow), and is enriched by extracted oil. Therefore, in the beginning of the cycle, the miscela is weak and then becomes concentrated at the extractor outlet. The miscela, after crossing the wagons, accumulates in trays 9 and then enters into another percolation section (through pumps and distributors), and the cycle is repeated. In the drainage zone 12, weak miscela abandons the spaces  $\varepsilon_b$  of the flakes.

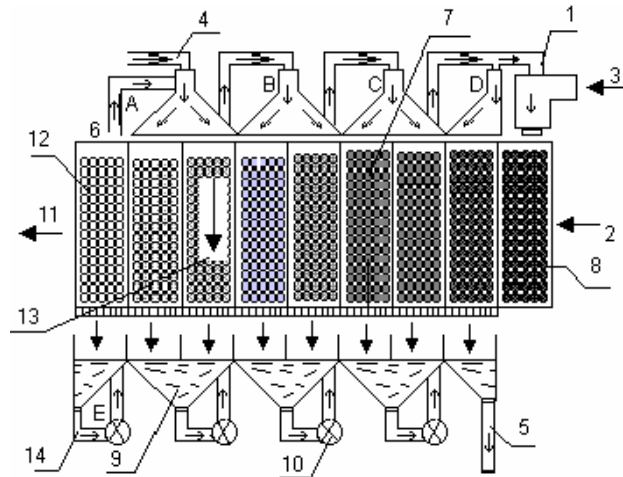


Figure 1. Main scheme of a “Rotocell.” extractor 1 - Miscela inlet in the loading section; 2- Inlet of wagons; 3- Inlet of flakes; 4-Solvent tube; 5-Concentrated miscela outlet; 6-Drained wagon; 7- Wagon in percolation section; 8-Wagon in loading section; 9-Miscela trays; 10-Pumps; 11- Outlet of flakes; 12-Drainage section; 13- Miscela flow inside the wagon; 14-Miscela flow after drainage; A, B, C, D-Miscela distributors.

## 2. Mathematical modeling

The aim of the model is to predict: two-dimensional ( $x$ - and  $z$ -directions) distribution of concentrations  $C$  e  $C^p$  in the extraction field in both stationary and transient regimes; oil losses (in outlet 11, Fig. (1)); oil concentration in the extractor outlet 5. In this case, the model should consider: the miscela and raw material flows in CCC pattern; oil transfer between solid, pore and bulk phases; the drainage and loading stages; the existence of trays and wagons with impermeable lateral walls; oil distribution particularities on wagon surfaces; the division of extraction field into percolation sections; oil diffusion throughout the bulk phase; the possibility of the miscela overflowing from a wagon into two different trays at the same time.

The physical scheme created in these conditions includes the following considerations:

1. The extraction field is formed by a group of percolation sections, with the miscela flow in the vertical direction and motion of the wagons with flakes in the horizontal direction.
2. Each wagon is represented by a group of vertical columns (Fig. (2)) having width  $\Delta x$ , and the uniform raw material flows in batch periods. These periods are defined by the formula:  $\Delta t = \Delta x/u$ , where  $u$  is the wagon horizontal speed.
3. An analysis of experimental data (Karnofski, 1986) and of the extractor operational regime (Moreira et al, 1999) shows that, together with the exit oil from the solid and pore phases, an opposite transfer of solvent in almost equivalent volume occurs. With this assumption, the miscela volumetric flow in the extractor ( $Q_T$ ) is constant and does not depend on the processes of oil transfer between the phases.
4. It is supposed that the operational regime is transient and that the concentrations  $C$  and  $C^p$  in the extraction field and in the loading and drainage zones vary with the time.
5. In the upper part of each column, enters the miscela that escapes from the previous percolation section.
6. Diffusion is only considered along each column.
7. In loading zone, the miscela of the  $(m_s+1)$ -th tray occupies the spaces  $\varepsilon_b$  between the particles and part of the spaces  $\varepsilon_p$  inside the particles.
8. During the raw material loading, the equilibrium between the concentrations in solid ( $C^N$ ) and pore ( $C^p$ ) phases is established, that is maintained during the whole extraction process. The volumetric equilibrium constant ( $E_d^v$ ) is defined by the formula:

$$E_d^v = \frac{C^N}{C^p} = E_d \left[ \frac{\rho_s}{\rho_{he} + C^p(\rho_{ol} - \rho_{he}) + E_d C^p(\rho_s - \rho_{ol})} \right] \quad (1)$$

which can be obtained by the formula  $E_d = g_N / g_p$  replacing the mass fractions ( $g_N, g_p$ ) by the volumetric fractions ( $C^N, C^p$ ), where  $\rho_{he}, \rho_{ol}$  and  $\rho_s$  are the hexane, oil and solid phase densities, respectively.

9. Outside the extraction field, the mass transfer between the pore and bulk phases do not occur.

10. In the drainage zone, every bulk phase passes through the solvent inlet. The oil contained in the pore and solid phases is considered lost.

11. The horizontal area  $A_v$  of the wagons is constant. For this reason (considering that the flow  $Q_T$  is constant), the vertical miscela velocity  $V_m$  is also constant.

12. In the trays, the oil concentration is uniform, but changes with time.

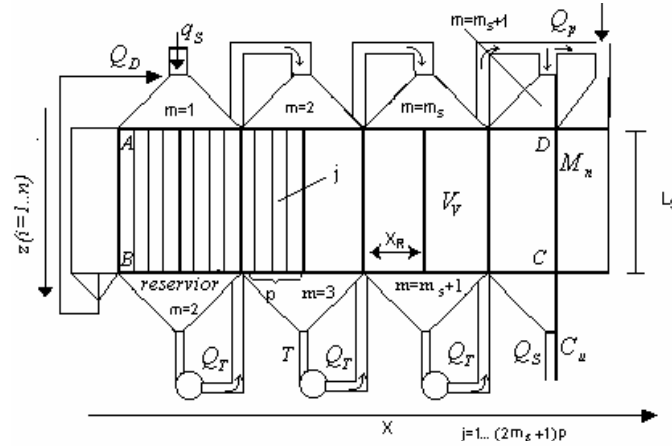


Figure 2. Extractor dimensional scheme for the mathematical model,  $ABCD$  – extraction field;  $A$  – coordinates origin ( $z, x$ );  $V_v$  – wagon volume;  $L_S$  – wagon height;  $X_R$  – wagon average width.

In Figure (2) an outline of the extractor dimensions is presented. Two wagons correspond to one percolation section and the last section to just one. The model components of the extraction field are numbered from the left to the right, to know: the wagons of  $1$  up to  $2m_s+1$ ; the sections from  $1$  up to  $m_s+1$ ; the columns from  $1$  till  $M_C=(2m_s+1)p$  (where  $p$  is the number of the wagon columns) and the trays from  $2$  to  $(m_s+1)$ .

Because of the use of two time scales (continuous and discrete according to the assumption 2), the artificial neural networks (RNA) approach is applied in this work in combination with the flow continuous model. This approach is a concept that was developed for biological models, and later it found many applications in engineering areas, for instance, (Nikravesh et al, 1997; Azevedo et al, 2000; etc). In the RNA scheme, some original concepts are used: neuron, outlet function, activation function, discrete time, training of connections, etc. The elaboration of the mathematical models through RNA enables the application of the same models not only in design but also in the operational control of real facilities. However, to conceive the mathematical model in the form of RNA, it is necessary to build up sub-models of some extractor components in continuous flow terms. The main sub-models are:

**Extraction field sub-model.** The extraction field  $ABCD$  is composed by  $M_C$  virtual columns with width  $\Delta x$ ; processes inside the  $j$ -th column are described by the equations presented in Majundar et al (1995), which are modified in accordance with the assumption adopted in the physical scheme:

$$\frac{\partial C_j}{\partial \tau} = -\frac{V_m \partial C_j}{\partial z} + E_s \frac{\partial^2 C_j}{\partial z^2} + \left( \frac{1 - \varepsilon_b}{\varepsilon_b} \right) k_f a_p (C_j^p - C_j); \quad j=1 \dots M_C; \quad (2)$$

$$\frac{\partial C_j^p}{\partial \tau} = -\frac{k_f a_p}{\varepsilon_p + (1 - \varepsilon_p) E_d^v} (C_j^p - C_j); \quad (3)$$

where  $E_s$  – the dispersion coefficient that was determined by formula:  $E_s = 0,7D_{AB} + 2,0V_m d_p$ , found at (Cussler, 1997). Sherwood number ( $Sh$ ) to define the coefficient  $k_f$  is found in (Treybal, 1963):

$$a) \quad Sh = 2,4 Re^{0,34} Sc^{0,42} \quad \text{in} \quad 0,08 < Re < 125; \quad (4)$$

$$b) \quad Sh = 0,442 Re^{0,69} Sc^{0,42} \quad \text{in} \quad 125 < Re < 5000; \quad (5)$$

The Equations (2) and (3) for  $j$ -th column are linked to the equations for other columns through boundary conditions. Concentration equations in trays. The equation for the  $m$ -th tray situated under the extraction field is derived (considering the hypothesis 12) from the conservation law for the oil species, and is given by:

$$\frac{d\bar{C}_m}{d\tau} = \frac{V_m A_v \varepsilon_b}{V_b} \left( \frac{1}{p} \sum_{j=2(m-2)p+1}^{j=2(m-1)p} C_j(L_S, \tau) - 2\bar{C}_m(\tau) \right); \quad m = 2 \dots m_S; \quad (6)$$

Drainage sub-model. The drainage sub-model includes formulas to determine: the drained flow ( $Q_D$ ), total flow ( $Q_T$ ), the average drained concentration ( $C_D$ ), the initial oil concentration in the solvent ( $C_{in}$ ) and oil loss ( $Q_{ol}^{pN}$ ). From the assumptions:

- drainage and total outpouring:

$$Q_D = \frac{V_v \varepsilon_b}{\Delta t_v}; \quad Q_T = Q_D + q_s; \quad (7)$$

- oil loss:

$$Q_{ol}^{pN} = \frac{V_v (1 - \varepsilon_b) [\varepsilon_p + (1 - \varepsilon_p) E_d^v]}{\Delta t_v L_S} \int_0^{L_S} C_j^p(z, \tau) dz; \quad j=1; \quad (8)$$

where  $\Delta t_v = X_R/u$  is the time of a wagon entrance in the extraction field.

- the equation for concentration  $C_D$ :

$$\frac{dC_D}{d\tau} = \frac{Q_D}{L_S V_D} \int_0^{L_S} C_j(z, \tau) dz - \frac{Q_D C_D}{V_D}; \quad (9)$$

where  $V_D$  is the volume to collect drained miscela.

Oil concentration in the first section entrance ( $C_{in}$ ) is related to the concentration  $C_D$  (according to Fig. (2)) by:

$$C_{in} = \frac{C_D Q_D + C_{in}^{he} q_s}{(q_s + Q_D)}; \quad (10)$$

Loading sub-model. The purpose of this sub-model is to determine the initial oil concentration in the pore phase ( $C_{in}^p$ ) as well as the miscela flow ( $Q_p$ ) that is necessary to fill out the spaces ( $\varepsilon_b, \varepsilon_p$ ) in the raw material located in the loading zone (wagon 8, Fig. (1)). Raw material in extractor inlet contains the oil only in the solid phase with initial mass concentration ( $N_i$ ) and the volumetric concentration  $C_e$  defined by formula:

$$C_e = \frac{N_i M_n}{V_v \rho_{ol} (1 - \varepsilon_p) (1 - \varepsilon_b)}; \quad (11)$$

where,  $M_n$  – raw material mass inside a wagon.

In the sub-model, it is considered that the concentrated miscela (with concentration  $\bar{C}_{m_s+1}$ ) fills out the spaces (Fig. (3a)) between the flakes (forming the bulk phase) and soaks in the flakes (that have porosity  $\varepsilon_p$ ), occupying part of the pores ( $\varepsilon_m$ ).

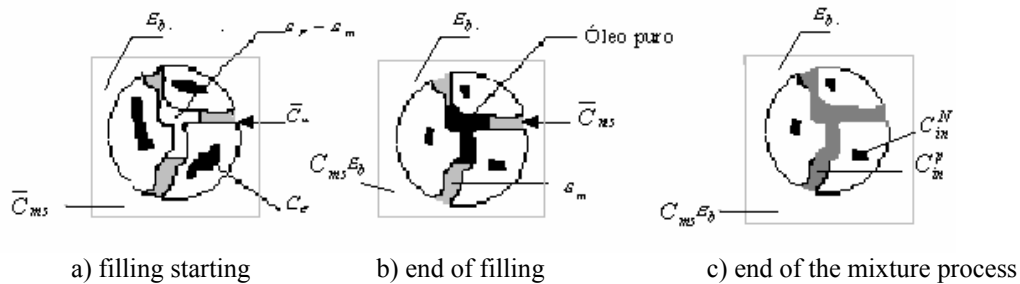


Figure 3. Scheme of pore phase filling.

At the same time, due to the extraction force, the solid phase oil comes out to the phase pore, occupying the other part of  $\varepsilon_p$  with an equivalent amount of  $\varepsilon_p - \varepsilon_m$  (Fig. (3b)). After this process, the uniform oil mixture is quickly set up in these spaces and, as a result, a concentration  $C_{in}^p$  (Fig. (3c)) is formed. It is also assumed that some amount of oil ( $C_{in}^N$ ) continues in the solid phase and it is in equilibrium with the pore phase ( $C_{in}^p$ ).

This process is described by equations:

- total oil balance in the solid and pore phases between stages a) and c):

$$C_e(1 - \varepsilon_p) + \bar{C}_{m_{s+1}}\varepsilon_m = C_{in}^p\varepsilon_p + C_{in}^N(1 - \varepsilon_p) \quad (12)$$

- equilibrium in the stage c)

$$C_{in}^N = E_d^v C_{in}^p \quad (13)$$

- oil balance in the pore phase between stages b) e c):

$$\varepsilon_p - \varepsilon_m + \bar{C}_{m_{s+1}}\varepsilon_m = C_{in}^p\varepsilon_p \quad (14)$$

The formula to calculate  $C_{in}^p$  follows directly from the above equations:

$$C_{in}^p = \frac{C_e(1 - \varepsilon_p) + \bar{C}_{m_{s+1}}\varepsilon_p}{\frac{\bar{C}_{m_{s+1}}\varepsilon_p}{1 - \bar{C}_{m_{s+1}}} + \varepsilon_p + E_d^v(1 - \varepsilon_p)}; \quad (15)$$

Formula to define  $Q_p$  was assumed considering that miscela of concentration  $\bar{C}_{m_{s+1}}$  fulfills spaces  $\varepsilon_b$  and  $\varepsilon_m$ :

$$Q_p = \frac{V_v}{\Delta t_v} \left[ \varepsilon_b + (1 - \varepsilon_b) \frac{\varepsilon_p(1 - C_{in}^p)}{(1 - \bar{C}_{m_{s+1}})} \right]; \quad (16)$$

Miscela oil concentration in extractor outlet  $C_u$  is determined by formula:

$$C_u(\tau) = \frac{1}{p} \sum_j C_j(z, \tau) \quad j = (M_C - p + 1) \dots M_C; \quad (17)$$

**Boundary conditions.** According with design of the counter-current crossed flows, (Fig. (2)) the boundary conditions for the equations in each column are:

$$C_j(z, \tau) = \bar{C}_{in}(\tau); \quad \text{for } j = 1 \dots 2p; \quad z=0; \quad \tau \geq 0; \quad (18)$$

$$C_j(z, \tau) = \bar{C}_m(\tau); \quad \text{for } j = (2p(m-1)+1) \dots 2pm; \quad m = 2 \dots m_s; \quad z = 0; \quad \tau \geq 0; \quad (19)$$

$$C_j(z, \tau) = \bar{C}_{m_{s+1}}(\tau); \quad \text{for } j = (2pm_s+1) \dots M_C; \quad z = 0; \quad \tau \geq 0; \quad (20)$$

$$\frac{\partial C_j(z, \tau)}{\partial z} = 0; \quad \text{for } j = 1 \dots M_C; \quad z = L_s; \quad \tau \geq 0; \quad (21)$$

### 3. Model in terms of artificial neural networks

The aforementioned sub-model group acts continuously in each time interval  $\Delta t$  when the raw material is motionless. Between the intervals  $\Delta t$ , an instantaneous displacement in distance  $\Delta x$  occurs i.e. the content of the  $j$ -th column (miscela and flakes) is replaced by the content of the  $(j+1)$ -th column. These displacements are shown in Fig. (4) (stippled lines), where the extractor outline is shown in terms of RNA. The solid lines in this net reflect the continuous transfers. The net is heterogeneous (it includes several types of neurons), complex (it includes a subsystems of neurons), and dynamical (with two time scales: continuous and discrete). In Figure (4), each neuron, block of neurons and connections between them reflect some component of the physical scheme. The equations that describe the states, inlets, outlets, and activation functions form the extractor mathematical model.

In particular: Neuron  $N_1$  corresponds to the solvent inlet with parameters:  $q_s, C_{in}^{he}$ . Neuron  $N_2$  corresponds to the raw material inlet with parameters:  $(M_v/\Delta t_v), N_t$ . Neuron  $N_3$  corresponds to the concentrated miscela outlet with parameters:  $Q_s, C_u$ . Neuron  $N_4$  corresponds to the marc outlet with parameter:  $Q_{ol}^{pN}$ .

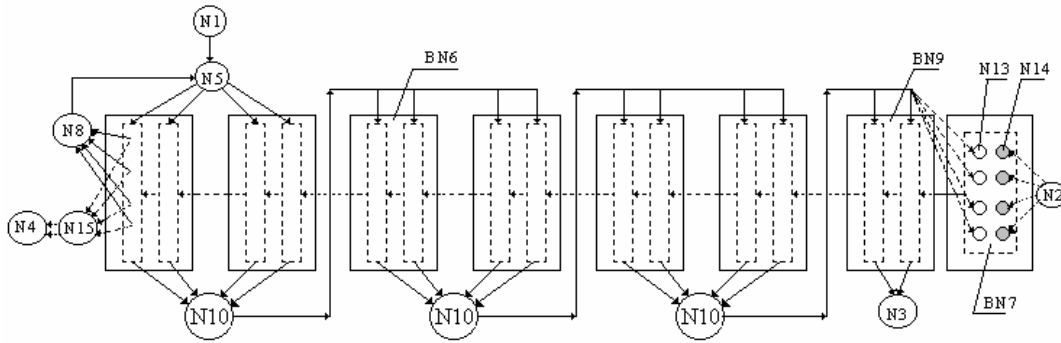


Figure 4. Extractor scheme in RNA form

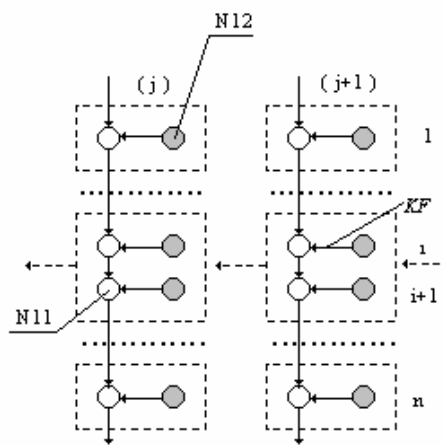


Figure 4a. BN6 block fragment

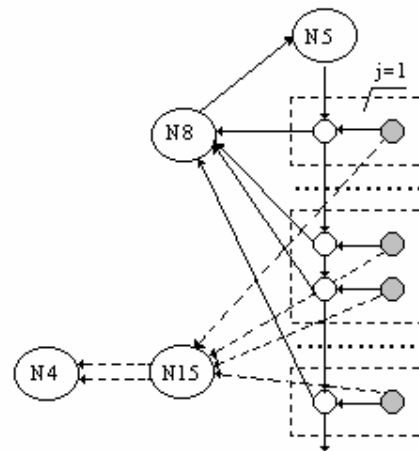


Figure 4b. RNA fragment of drainage zone

Neuron blocks BN6 reflect the processes in column and each one includes  $n$  neurons of the types  $N_{11}$  and  $N_{12}$  using space discretization ( $i = 1 \dots n$ ) of Eq. (2, 3), forming the activation function of type ODE for each neuron in extraction field. Neurons  $N_{11}(i, j)$  and  $N_{12}(i, j)$  are in  $i$ -th cell of  $j$ -th column. Each neuron  $N_{11}$  holds two inlets and two outlets. The neurons  $N_{11}(n, j)$  located in the bottom of each block BN6 deliver the information to the neurons  $N_{10}(m+1)$ , while the upper neurons in the same block obtains the information from the neurons  $N_{10}(m)$ . A wagon is represented in the RNA scheme by  $np$  neurons of the type  $N_{11}$  e  $N_{12}$ . The block of neurons BN7 corresponds to the loading zone and includes neurons  $N_{13}$  ( $i=1 \dots n$ ) e  $N_{14}$  ( $i=1 \dots n$ ). Each neuron  $N_{13}$  reflects the bulk phase and has one discrete inlet and two discrete outlets. Each neuron  $N_{14}$  corresponds to the pore phase in the loading zone, and has two inlets and one discrete outlet.

The calculation algorithm is determined by properties of the mathematical model in RNA terms; that is, in the intervals  $\Delta t$ , the evolution of neuron states is determined by continuous connections and is described by activation function; in the interval limits  $\Delta t$ , there are instantaneous alterations of the states induced by discrete connections that are equal to the changes of the ODE initial conditions. Then, the algorithm includes two alternate fragments:

- Integration of the ODE's in the first interval  $\Delta t$ ;
- Alteration of the ODE initial conditions;
- Integration of the ODE's in the second interval  $\Delta t$ ;
- Alteration of the ODE initial conditions, and so on until the end of the integration

The EDO's system is integrated by Runge-Kutta explicit method of the 4th order and 4 stages.

#### 4. Model and code verification

Mathematical model and code (ROTO1) were verified through:

- a) alteration of elementary cell sizes;
- b) test of the oil species conservation law;
- c) comparison with experimental data.

The data for verification of the numerical simulations (Tab. (1)) were chosen based on the real characteristics of Rotocell extractor, solvent and raw material that were taken from (Majundar et al, 1995; Moreira et al, 1999; Cussler, 1997; Treybal, 1963):

Table 1. Data for numerical simulations

$n$	$P$	$m_S$	$\Delta t_v$ (s)	$D_{AB} \cdot 10^9$ ( $m^2/s$ )	$q_s \cdot 10^3$ ( $m^3/s$ )	$\rho_{ol}$ ( $kg/m^3$ )	$E_d^v$	$\rho_s$ ( $kg/m^3$ )	$M_n$ (kg)
30	10	7	150	1.3	12.5	914.8	0.36	1180	1784
$A_v(m^2)$	$V_b(m^3)$	$L_S(m)$	$a_p$ (1/m)	$N_t$ (%mass)	$d_p(m)$	$\varepsilon_b$	$\varepsilon_p$	$C_{in}^{he}$	$\rho_{he}$ ( $kg/m^3$ )
1.56	0.2	2.3	57	18	0.005	0.4	0.3	0.001	661.68

The miscela properties  $\mu_m$  (Pa·s),  $\rho_m$  are functions of concentration, and are described by polynomials:

$$\mu_m \cdot 10^4 = 55,7C^2 - 0,73C + 3,73 ; \quad (22)$$

$$\rho_m = -35C^2 + 261,28C + 661,68 ; \quad \text{for } C \leq 0,4 ; \quad (23)$$

that were obtained by interpolating the data found in (Othmer & Agarwal, 1955).

The size of cells is controlled by the number  $n$  (number of horizontal layers in extraction field), and  $p$  (quantity of columns in a wagon). The integration step was determined by formula  $h = \Delta t/3$ . To avoid calculus divergence, it is necessary to assure Courant number in the vertical direction:

$$S_v = \frac{V_m h}{\Delta z} < 1; \quad (24)$$

In stationary state oil flows in extractor inlets and outlets have to obey the following relation:

$$\frac{N_t M_n}{\rho_{ol} \Delta t_v} + C_{in}^{he} q_s = Q_S C_u + Q_{ol}^{pN}; \quad (25)$$

Numeric simulations (se  $S_v < 1$ ) showed that the Eq (25) is satisfied with a relative precision:

$$\delta_f = 1 - \frac{(Q_S C_u + Q_{ol}^{pN}) \rho_{ol} \Delta t_v}{N_t M_n + C_{in}^{he} q_s \rho_{ol} \Delta t_v} \approx 0,1\% \quad (26)$$

From RNA point of view net training was accomplished by  $KF$  connections (Fig. (4a)) i.e. by mass transfer between pore and bulk phases. The training takes place through direct modeling (Azevedo, 2000) comparing the outlet signals between RNA (mathematical model) and 'supervisor' (experimental data). As outlet signal, the total oil loss ( $Q_{ol}^{pN}$ ) is chosen. As trained parameter the specific contact area  $a_p$  was applied. In the result, it was determined that  $a_p \approx 57$  (1/m) when the total loss in the model:

$$P_{ol}^t = \frac{(Q_{ol}^{pN}) \rho_{ol} \Delta t_v}{(1 - N_t) M_n} \quad (27)$$

coincided with the loss observed in the real extractor ( $P_{ol}^{ex} \approx 0,5\%$ )

The results obtained for the stationary state through our model and through method of ideal stages were compared (Fig. (5)) with experimental data collected in the company (Moreira et al, 1999). The concentrations in this method were calculated by Kremer-Souders-Brown formulas (Foust et al, 1982). As seen, both models predict satisfactory results in the first stages, but for reservoirs 6 and 7 the ideal stages method leads to concentrations  $\bar{C}_m$  that are quite different from the experimental data. It is necessary to stress two aspects:

- the method of ideal stages leads to the same results independently of the parameters  $L_S, \Delta t_v, X_R, \varepsilon_b$ , etc., when, in reality, distributions  $\bar{C}_m$  depend on the alteration of these parameters;

- the model developed in this work is sensitive to the changes in the extractor parameters and in the raw material characteristics. Besides, it predicts the concentration space distribution in the extraction field that is shown in the next section of the work.

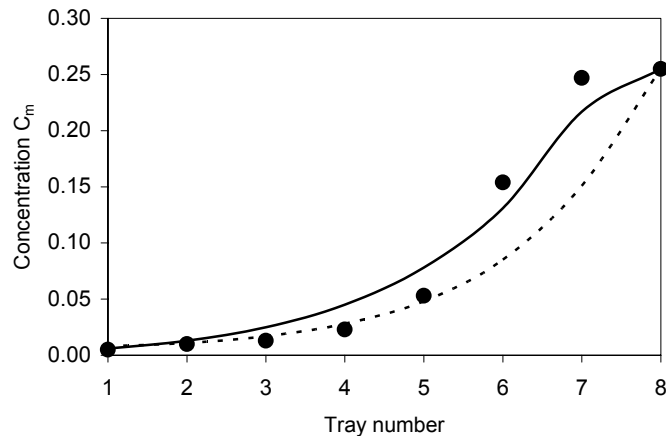


Figure 5. Distribution of concentrations  $\bar{C}_m$  along the extractor: — Code; - - - Ideal stages; • Experimental data.

## 5. Numerical simulation

The numerical simulation of the transient regime till the establishment of steady regime of field was performed for data of Tab. (1), with initial uniform and different concentrations  $C(z) = \bar{C}_m = 0,01$ ;  $C^p(z) = 0,2$ . The results are shown in Figs. (6-9) in the form of three-dimensional plots  $C = f(x, z)$ ;  $C^p = f(x, z)$ . The solvent inlet zone (miscela with concentration  $C_{in}^{he} \approx 0,001$ ) in extractor (tube 4 Fig. (1)) corresponds to coordinate:  $x = 0...6$ ;  $z = 0$  and concentrated miscela outlet zone (tube 5 Fig. (1)) to coordinates:  $x = 48..51$ ;  $z = 30$ . For the raw material inlet and outlet zones, the coordinates are, respectively:  $x = 51$ ,  $z = 0\div30$ ; and  $x = 0$ ,  $z = 0\div30$ .

Figures (6a, 6b) for time  $\tau = 75s$  show that, in the extractor inlets, the initially uniform concentration field started to deform. It is shown the existence of a concentration wave on one side of the extractor, (Fig. (6a)) while on the other side an abrupt front of high concentration  $C^p$  (Fig. (6b)) emerged from the loading zone. In most of the extraction field, it is observed a growth of concentrations  $C$  and a decrease of  $C^p$  due to the fast oil transfer between the pore and bulk phases ( $C(x, z) \approx 0,03$ ;  $C^p(x, z) \approx 0,17$ ).

The extraction field in time  $\tau = 750s$  is presented in Fig. (7a, 7b). The plot  $C = f(x, z)$  shows waves passing through the second and third sections, and forming steps between the sections ( $x = 12$ ;  $z = 0...30$ ). The step corresponding to  $x = 6$ ,  $z = 0...30$  is steeper, because, in the oil distribution of the first section, it strongly affected the initial concentration  $C_{in}$ . In the other end, the front is moved forming, in  $x = 42...50$ ,  $z = 0...30$ , a region of high concentration with a step (corresponding to  $x = 48$ ,  $z = 0...30$ ) between the last two sections.

In the distribution of  $C_j^p = f(x, z)$ , the pattern of front displacement and of concentration increase continues. In the first sections, the concentration distribution  $C^p = f(x, z)$  presents a slope due to the decrease in the concentrations  $C$ . In the central region of the extraction field, the concentrations approximate each other, being almost the same ( $C(z) \approx 0,07$ ;  $C^p(z) \approx 0,09$ ). In the plot for  $C = f(x, z)$ , it can be seen the formation of three steps between the first sections and two steps in the last sections. They are more perceptible on the tops ( $z = 0$ ) than on the bottoms ( $z = 30$ ) of the sections because of the miscela diffusion and its displacement in the horizontal direction. In the bottom of the last section ( $x = 48...51$ ,  $z = 30$ ), a maximum of  $C \approx 0,18$  is created.

In time  $\tau = 975s$  (Fig. (8a, 8b)), the distribution  $C = f(x, z)$  was still characterized by the the same trends:

- almost all steps between the sections were already formed, with the heights of the first steps decreasing and the heights of the last steps increasing;
- the maximum concentration in the last section increased ( $C = 0,21$ );
- the "plateau" almost disappeared, except in the center of the field.

In the plot  $C^p = f(x, z)$ , the wave front moved in the central part of field and almost disappeared, but the "slope" height increased. The trend of decrease in  $C^p$  of the first sections continued.

In Figures (9a, 9b), the distributions  $C = f(x, z)$  e  $C^p = f(x, z)$  are shown in time  $\tau = 3600s$ , which is closer to the stationary state. All steps are already formed (Fig. (9a)), with the heights approximately corresponding to the method of ideal stages but with concentration spatial distributions, where are observed: smooth in section bottoms, existence of maximum in last section, etc. The "plateau" observed in time  $\tau = 975s$  completely disappeared.

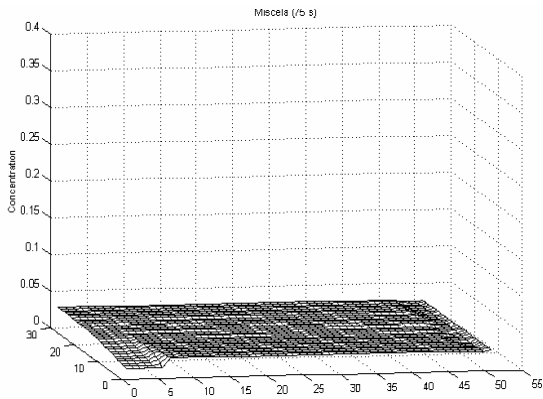


Figure 6a. Phase bulk, time = 75s.

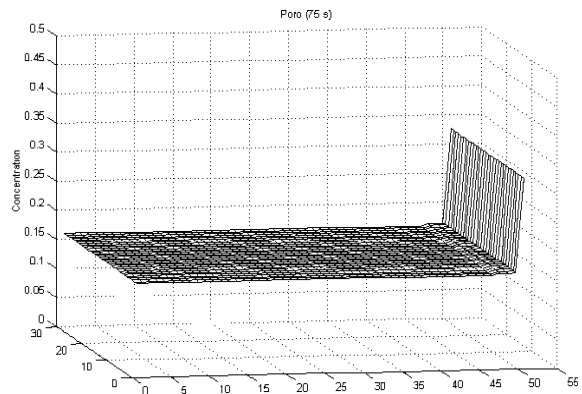


Figure 6b. Phase poro, time = 75s.

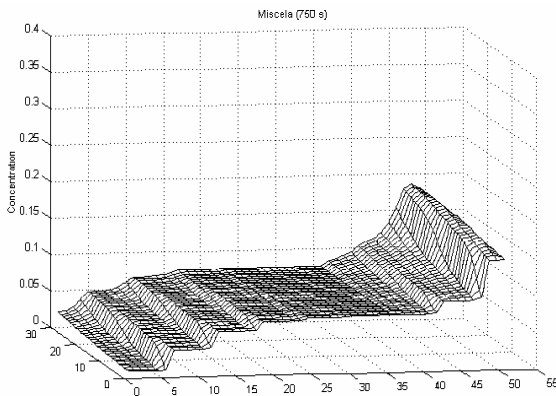


Figure 7a. Phase bulk, time = 750s.

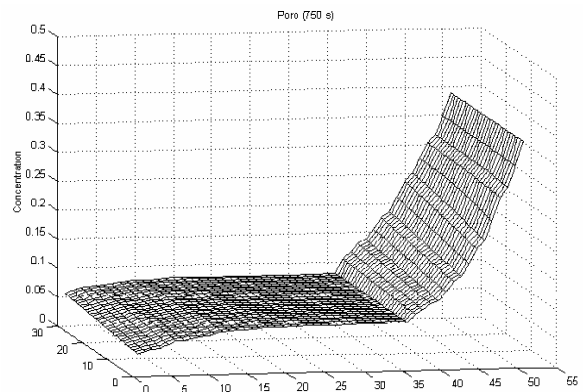


Figure 7b. Phase poro, time = 750s.

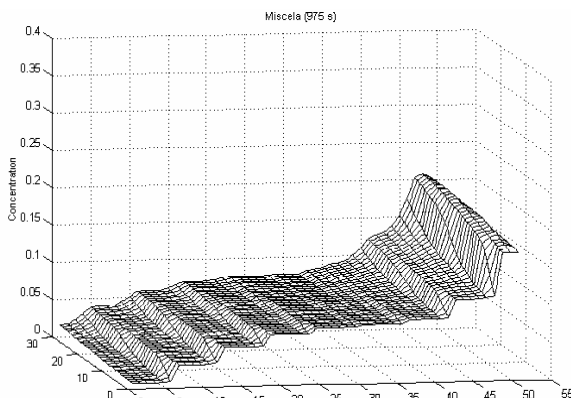


Figure 8a. Phase bulk, time = 975s.

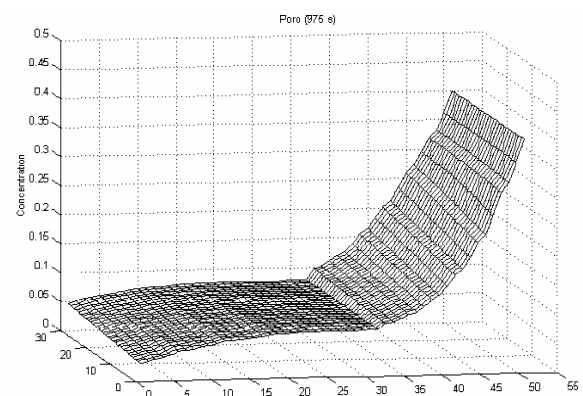


Figure 8b. Phase poro, time = 975s.

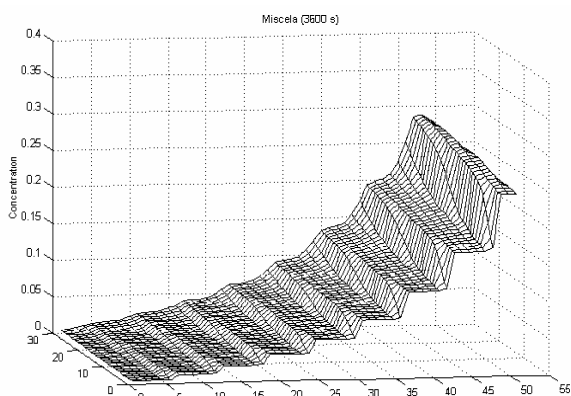


Figure 9a. Phase bulk, time = 3600s.

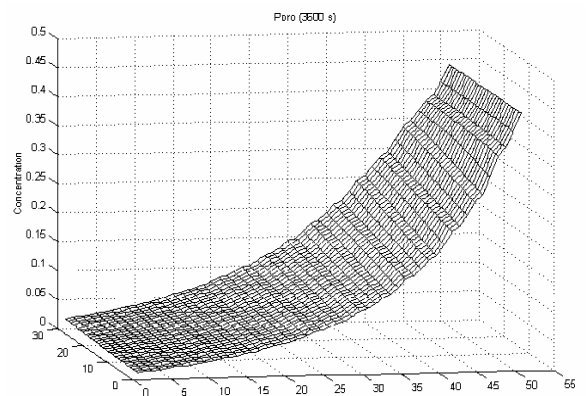


Figure 9b. Phase poro, time = 3600s.

The distribution  $C^p = f(x,z)$  established only a monotonic concentration gradient. However according to the method of ideal stages, the concentrations  $C^p$  should present steps between sections that do not correspond to the distribution  $C^p$  of actual extractors. The numerical simulations show that the stationary state is obtained in  $\tau = 12600$ s. It is discernible that, during time interval  $\Delta\tau = 12600 - 3600 = 9000$ s, distributions  $C = f(x,z)$  e  $C^p = f(x,z)$  practically do not change.

## 6. Conclusion

In this work a new model was developed for counter-current crossed flows applied in an industrial extractor "Rotocell." The proposed model is a two-dimensional, transient one and considers the main phenomena that involved in the extractor: mass transfer between the bulk and pore phases, oil diffusion through bulk phase, existence of trays, and the influence of drainage and loading zones on its operational characteristics. The new model was sensitive to: the raw material properties, the extractor operational parameters, and the section dimensions.

It includes the sub-models: for the extraction field, trays, drainage and loading. These sub-models are transformed in form of RNA that could: allow with simplicity the use of two time scales (continuous and discrete), accomplish training of connections, and apply the model to the design and control of the extractor. The RNA (besides the method of line) is one of the possible ways to reduce the PDE's of mathematical model up the ODE system, which is solved in this work by the Runge-Kutta method. The net training was accomplished by mass transfer connections in the extraction field between the pore and bulk phases, by adjusting the area of contact ( $a_p$ ).

The developed code could solve cases with up to 50000 ODE (the number of ODE was determined by the parameters  $n$  e  $p$  of the extraction field discretization). The algorithm was stable, without presenting oscillations with the mesh resolution. Comparison with experimental data and species conservation law (oil) showed a satisfactory accuracy of the solution, which allowed verifying both the model and the code.

The numerical simulations revealed several interesting effects that usually occur with the application of new, more detailed models. Among these effects, the following can be mentioned: the "waves" of concentrations passing through the sections, the formation of steps, the appearance and displacement of fronts with subsequent formation of slopes; formation and establishment of the maximum concentration, etc.

## 7. Acknowledgements

The authors thank CNPq for the financial support (process n°470458/2001-1) and companies Coimbra Clayton (Cruz Alta-RS) and Camera (Santa Rosa-RS) for the permission and technical assistance during investigation.

## 8. References

- Abraham, G., Hron, R.J. and Koltin, S.P., 1988, "Modeling the Solvent Extraction of Oilseeds", JAOCS, Champaign, January, Vol. 65, No. 1, pp.129-135.
- Azevedo, F.M., Brasil, L.M. and Oliveira, R.C.L., 2000, "Redes Neurais com Aplicações em Controle e em Sistemas Especialistas", Visual Book, Brazil.
- Bewaji A. and Best R.J., 1996, "Flow sheet Simulation of Coffee Extraction: A Continuous Cyclic Process", Computers Chem. Eng, Vol. 20, pp. S485-S490.
- Bockisch, M., 1998, "Fats and Oils Handbook", AOCS Press, Illinois, EUA.
- Cussler, E.L., 1997, "Diffusion: Mass Transfer in Fluid Systems", 2<sup>nd</sup> ed., Cambridge, University of Minnesota.
- Foust, S.A., Wenzel, A.L., Chump, W.C., Maus, L. and Anderson, B.L., 1982, "Princípio das Operações Unitárias", 2 edição, Ed. Livros Técnicos e Científicos, Brazil.
- Karnofsky, G., 1986, "Design of Oilseed Extractors", JAOCS, Campaign, Vol. 63, No. 8, pp.1011-1016.
- Majundar, G.C., Samanta A.N. and Sengupta S.P., 1995, "Modeling Solvent Extraction of Vegetable Oil in a Packed Bed", JAOCS, Campaign, Vol. 7, No. 9, pp. 971-979.
- Moreira L.G., Elias C.R. and Thomas G.C., 1999, Coleta de Dados Experimentais do Extrator Rotocell (Empresa Coimbra-Clayton) no Regime Estacionário, UNIJUI, Ijuí-RS, Brazil, 15p.
- Nikraves M., Farrell A.E. and Stanford T.G., 1997, "Dynamic Neural Network Control for Non-linear System: Optimal Neural Network Structure and Stability Analysis", Chemical Engineering Journal, Vol. 68(1), pp. 41-50.
- Othmer, D.F. and Agarwal, J.C., 1955, "Extraction of Soybeans", CEP New York, Augusta, pp.372-378.
- Treybal, R.E., 1963, "Liquid Extraction", 2<sup>nd</sup> ed., McGraw-Hill, Series in Chemical Engineering, New York.